Journal of Low Temperature Physics, Vol. 146, Nos. 3/4, February 2007 (© 2007)
DOI: 10.1007/s10909-006-9275-8

Influence of Normal Fluid Disturbances on Interactions of Solid Particles with Quantized Vortices

Y. A. Sergeev,[1] S. Wang,[1] E. Meneguz,[2,3] and C. F. Barenghi[4]

[1]*School of Mechanical and Systems Engineering, Newcastle University, Newcastle upon Tyne NE1 7RU, UK*
E-mail: yuri.sergeev@ncl.ac.uk
[2]*Facoltà di Ingegneria, Università degli Studi di Udine, 33100 Udine, Italy*
[3]*Dipartimento di Energetica e Macchine, Università degli Studi di Udine, 33100 Udine, Italy*
[4]*School of Mathematics, Newcastle University, Newcastle upon Tyne NE1 7RU, UK*

(Received September 11, 2006; revised November 27, 2006)

Two-dimensional Lagrangian trajectories of the inertial particle in helium II are analyzed in the vicinity of the triple-vortex structure, i.e. the superfluid vortex and the normal dipole-like vortex structure induced by the mutual friction. It is shown that the vortices in the normal fluid can deflect the particle which otherwise would have collided with the superfluid vortex and, provided that the relative velocity of the particle and the vortex is not too large, would have been trapped by it. A geometrical impact parameter, which in the considered two-dimensional model, plays a rôle of the cross-section of particle–vortex collision, is determined and calculated as a function of temperature, externally applied superfluid velocity, and the Stokes number defined by the size of the local vortex structure, superfluid line velocity, and particle viscous response time.

***PACS Numbers**: 67.40.Vs Quantum fluids: vortices and turbulence; 47.80.+v Fluid mechanics: instrumentation for fluid mechanics; 47.27.-i Fluid mechanics: turbulent flows.*

1. INTRODUCTION

PIV (Particle Image Velocimetry) was, for many years, perhaps the most popular tool of flow visualization in classical fluid dynamics, but only recently was it implemented in liquid helium.[1,2] This technique is based on tracking small (usually micron-size in He II measurements) particles. Somewhat naively, one might expect that at temperatures between 1 K and $T_\lambda \approx 2.17$ K, where both the superfluid and normal components

of He II are present, the viscous drag exerted on the particle by the normal fluid dominates all other forces so that small particles should trace the normal component of superfluid helium. However, at sufficiently small distances between the particle and the core of the superfluid vortex, the latter generates a large pressure gradient force; in the presence of particle, the vortex itself bends and can reconnect to the particle surface, so that the particle can, eventually, be trapped on the superfluid vortex line (a similar scenario for trapping of ions by a vortex line in a Bose–Einstein condensate was discussed by Berloff and Roberts.[3]) Some of the recent PIV data[1,2] indicate a possibility of particle trapping or, at least, strong particle–vortex interaction. Preliminary, rather qualitative theoretical considerations of particle–vortex interactions (and particle trapping in particular) were given in our recent paper[4] based on the equations, derived in the cited paper, of motion of the inertial particle in He II.

The scenario described above suggests that the superfluid vortex traps any particle which happens to be in a sufficiently close vicinity of the vortex core, provided that the particle velocity relative to the vortex is not very high. However, this mechanism ignores any disturbances which a moving superfluid vortex induces in the normal fluid. Our concern is the effect of these normal fluid disturbances on a tracer particle which approaches the superfluid vortex line. In particular we want to find if the disturbances can deflect the inertial particle which otherwise would have collided with the superfluid vortex.

The existence of such disturbances is a consequence of the mutual friction force discovered by Hall and Vinen.[5] Unfortunately there is no direct experimental evidence of their nature. The only information arises from the numerical investigations of Idowu *et al.*[6] and Kivotides *et al.*[7] Using a two-dimensional model, Idowu *et al.* determined numerically the perturbation that a straight superfluid vortex filament (vortex point in 2D) induces in the normal fluid. They found that the flow of the normal fluid in the vicity of the superfluid vortex line resembles a dipole with a localized jet structure formed in response to the mutual friction force, see Figs. 1A and D in their paper.[6] Their result was confirmed by Kivotides *et al.*[7] who performed a fully three-dimensional numerical calculation of the motion of a single superfluid ring in which normal fluid and superfluid affected each other via the mutual friction force in a fully self-consistent way. When considering these results,[6,7] it must be remembered that in all other existing numerical investigations the normal fluid velocity field is prescribed and the mutual friction force affects only the superfluid vortices; for example, imposed uniform,[8] Poiseuille,[9] Gaussian[10] and ABC[11] normal fluid profiles are discussed in the literature.

In this paper, based on the equations[4] we analyze two-dimensional Lagrangian trajectories of the solid particle in the vicinity of the two-dimensional triple-vortex structure. We adopt here a simplest model of the particle–vortex interaction assuming that the presence of the particle modifies neither the motion of the superfluid vortex nor the normal flow. The flow field in the normal fluid is modeled by a simple analytical streamfunction which represents the main features of the numerical solution.[6] We found that, indeed, the normal vortices can deflect the particle which otherwise would have collided with (and, possibly, trapped by) the superfluid vortex. We also calculated an impact parameter, defined as a critical distance between the particle and the axis of motion of the superfluid vortex line, as a function of temperature, externally applied superfluid velocity, and the parameters characterizing the properties of helium II and the solid particle.

Based on the model,[7] particle interactions with the normal fluid disturbances induced by the mutual friction were also accounted for in our recent three-dimensional numerical calculations[12] of the superfluid vortex ring propagating against a particulate sheet. In agreement with the results of the present work, it was shown that the normal fluid disturbances sweep most of the particles away from the vortex core. However, in the cited work the mechanism of particle–vortex collisions was not analyzed in detail; the aim of paper[12] was somewhat different: To address the question whether a direct information about the instantaneous normal fluid velocity could be obtained by measuring the velocities of solid particles, and also to analyze some statistical properties of the particulate motion.

2. SUPERFLUID AND NORMAL FLOW FIELDS

The two-dimensional superflow field induced by an isolated straight vortex filament has, in cylindrical coordinates (r, θ, z), the form $\mathbf{v}_s = (0, \kappa/(2\pi r), 0)$, where $\kappa \approx 9.97 \times 10^{-4} \text{cm}^2/\text{s}$ is the quantum of circulation.

We assume here that the superfluid vortex is driven by an externally applied uniform superfluid velocity field $\mathbf{V}_s$. Let $\mathbf{V}_\ell$ be the velocity of the vortex line. If the temperature is low enough (typically less than 1 K) that the normal fluid can be neglected, the vortex line is advected by the superflow: $\mathbf{V}_\ell = \mathbf{V}_s$. At higher temperatures the mutual friction force will cause the vortex line to slip with respect to the superflow, $\mathbf{V}_\ell \neq \mathbf{V}_s$. The magnitude V_ℓ is a function of V_s and temperature T,[6] see Table I.[13,14]

So far only numerical results[6] are available for the streamfunction of the induced normal fluid flow, $\psi_n(x, y)$ introduced, in the reference frame

TABLE I

Velocity of the vortex line V_ℓ, cm/s.

V_s (cm/s)	$T = 1.3$ K	$T = 1.5$ K	$T = 1.8$ K	$T = 2.1$ K
0.01	0.00978	0.00954	0.00946	0.0113
0.1	0.0979	0.0960	0.0962	0.110
1	0.981	0.963	0.964	1.081

of the vortex system, by the relation

$$\mathbf{v}_n = \left(\frac{\partial \psi_n}{\partial y}, -\frac{\partial \psi_n}{\partial x} \right), \tag{1}$$

where

$$\psi_n = \psi_{nL} - V_l y \tag{2}$$

with ψ_{nL} being the normal flow streamfunction in the laboratory reference frame. Here and below, the origin of the system of coordinates (x, y) is the superfluid vortex core, and the axis Ox is chosen along the direction of the velocity of the superfluid vortex line $\mathbf{V}_\ell$.

The simplest model for the streamfunction of the normal fluid flow, which would reproduce the main features of numerical results,[6] can be suggested in the form

$$\psi_{nL} = \frac{\Gamma}{2\pi}(\ln \sqrt{R_+} - \ln \sqrt{R_-}), \tag{3}$$

where

$$R_\pm = x^2 + (y \pm a) + a^2 \xi, \tag{4}$$

a is the distance from the superfluid vortex point to the points of maximum vorticity of the vortex structure in the normal fluid (see Fig. 1 and cf Figs. 1A and D in Ref. 6), and ξ is the parameter which can be used for fitting the velocity distribution in the normal fluid calculated from Eqs. (3) and (4) with that obtained numerically.[6] In Eq. (3), Γ is the parameter, associated with a positive circulation Γ_+ in the normal dipole vortex structure, obtained by integrating the vorticity $\omega_n = -\nabla^2 \psi_n$ over the area $y > 0$ in which $\omega_n > 0$. From Eqs. (2)–(4) the positive circulation can be easily calculated as $\Gamma_+ = (\frac{1}{2} + \frac{1}{\sqrt{3}})\Gamma \approx 0.928\Gamma$. The circulation Γ_+ was found earlier[6] as a function of the externally applied superfluid velocity and temperature, $\Gamma_+ = \Gamma_+(V_s, T)$, see Table II.[13]

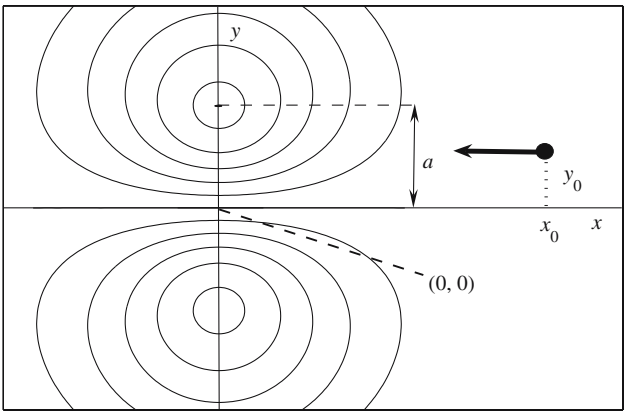

Fig. 1. Normal flow streamlines defined by the modeling streamfunction of Eqs. (3) and (4) in the laboratory reference frame. The superfluid vortex line which generates this dipole structure is located at the origin $x=0$, $y=0$ of the figure along the z axis.

TABLE II

Positive circulation in the normal fluid, $10^3 \times \Gamma_+$, cm^2/s.

V_s (cm/s)	$T=1.3$ K	$T=1.5$ K	$T=1.8$ K	$T=2.1$ K
0.01	0.0557	0.111	0.195	0.139
0.05	0.223	0.501	0.918	0.473
0.1	0.445	0.96	1.558	0.765

Idowu *et al.*[6] found that $a \approx 10^{-2}$cm for all temperatures and superfluid velocities. Since a and the circulation around one side of the normal vortex dipole are perhaps the main normal flow parameters affecting the motion of the solid particle in the vicinity of the vortex structure, for Γ_+ we will assume the values shown in Table II. The other two parameters that we would like to keep reasonably close to those calculated from numerical analysis[6] are the peak velocity, v_{n0}, and the normal fluid jet length, the latter being defined as the distance over which the normal velocity falls to 25% of the peak velocity. In the laboratory reference frame, the peak velocity calculated from the model (3)–(4) is

$$v_{n0} = \frac{\Gamma}{\pi a(1+\xi^2)}, \tag{5}$$

and the jet length $L = \sqrt{3}\xi a$. Below we choose $\xi = 1$. Then, for example, for $T = 1.8$K and $V_s = 0.1$cm/s ($\Gamma_+ = 1.558 \times 10^{-3}\,cm^2/s$) our sim-

ple model yields the peak velocity 0.027 cm/s and the jet length 0.017 cm. For the same T and V_s, the numerical results[6] give $v_{n0} \approx 0.039$ cm/s and $L \approx 0.03$ cm. In principle, the parameters of our model could be adjusted such that a, Γ_+, v_{n0} and L would all be within 20% of their respective values calculated in the cited work, although such an adjustment becomes impossible in the case where the temperature is very close to $T_\lambda \approx 2.17$ K. However, it should be stressed here that the numerical values of these quantities calculated in the cited work[6] were rather sensitive to the chosen size of the periodic box and boundary conditions, and, therefore, should themselves be regarded not as exact values but rather as estimates.

It was also shown by Idowu *et al.*[6] that the angle θ between the peak normal fluid velocity and the superfluid line velocity is not zero but depends on V_s and T, so that the triple-vortex structure does not necessarily move along the line of symmetry through the superfluid vortex core. However, this angle is not large (between 0.2π and -0.25π) for temperatures within the interval from 1.2 to 2.1 K. For the purpose of the following, rather qualitative analysis of particle interaction with the triple-vortex structure we will assume first that $\theta = 0$, and analyze briefly in Section 5 an influence of θ on the trajectories and trapping of solid particles.

3. LAGRANGIAN EQUATIONS OF PARTICLE MOTION

The dynamic equation of motion of a spherical Stokesian particle (such that the particle Reynolds number $\mathrm{Re}_p = 2\rho_n a_p |\mathbf{v}_n - \mathbf{u}_p|/\mu_n \ll 1$, where ρ_n is the normal fluid density, a_p the particle radius, $\mathbf{u}_p$ the particle velocity, and μ_n the viscosity of helium II), derived, under a number of assumptions, by Poole *et al.*[4] has the form

$$\frac{d\mathbf{u}_p}{dt} = \frac{1}{\tau}(\mathbf{v}_n - \mathbf{u}_p) + \frac{3\rho_n}{2\rho_o}\frac{D\mathbf{v}_n}{Dt} + \frac{3\rho_s}{2\rho_o}\frac{D\mathbf{v}_s}{Dt}, \tag{6}$$

where the particle response time and the effective density are, respectively,

$$\tau = \frac{2\rho_o a_p^2}{9\mu_n}, \quad \rho_o = \rho_p + \frac{\rho}{2}. \tag{7}$$

For neutrally buoyant particles $\rho_o = \frac{3}{2}\rho$. The properties of liquid helium, in particular the temperature-dependent viscosity μ_n, can be found e.g. in the work by Donnelly and Barenghi.[15] For particle sizes typical of PIV applications in He II, the particle response time lies in the interval from $\tau \approx 2.69 \times 10^{-5}$ s (for neutrally buoyant ($\rho_p = 0.145$ g/cm^3) particles of size $a_p = 10^{-4}$ cm at $T = 2.1$ K) to $\tau \approx 2 \times 10^{-2}$ s (for particles of size $a_p =$

10^{-3} cm and density $\rho_p = 1.1\,\mathrm{g/cm^3}$ at $T = 1.8\,\mathrm{K}$). In Eq. (6), the substantial derivatives are defined as

$$\frac{D\mathbf{v}_n}{Dt} = \frac{\partial \mathbf{v}_n}{\partial t} + (\mathbf{v}_n \cdot \nabla)\mathbf{v}_n, \quad \frac{D\mathbf{v}_s}{Dt} = \frac{\partial \mathbf{v}_s}{\partial t} + (\mathbf{v}_s \cdot \nabla)\mathbf{v}_s. \tag{8}$$

Equation (6) must be considered together with the kinematic equation

$$\frac{d\mathbf{r}}{dt} = \mathbf{u}_p, \tag{9}$$

where $\mathbf{r} = \mathbf{r}(t) = (x(t),\ y(t))$ should be regarded as a Lagrangian trajectory of the solid particle.

In the reference frame of the triple-vortex system, moving with the velocity $\mathbf{V}_\ell$ relatively to the laboratory reference frame, $\partial \mathbf{v}_n/\partial t = \partial \mathbf{v}_s/\partial t \equiv 0$, and the term $(\mathbf{v}_s \cdot \nabla)\mathbf{v}_s$ has the form of the radial pressure gradient force, i.e.

$$(\mathbf{v}_s \cdot \nabla)\mathbf{v}_s = \frac{\kappa^2}{8\pi^2} \nabla \left(\frac{1}{r^2} \right). \tag{10}$$

We introduce non-dimensional variables denoted below by the superscript (*), assuming a, V_ℓ and a/V_ℓ as the length, velocity and time scale, respectively. The non-dimensional streamfunction of the fluid flow,

$$\psi_n^* = \psi_{nL}^* - y^* \tag{11}$$

is defined by the relation $\psi_n = aV_\ell \psi_n^*$, so that the non-dimensional components of the normal velocity are $v_{nx}^* = \partial \psi_n^*/\partial y^*$ and $v_{ny}^* = -\partial \psi_n^*/\partial x^*$. In (11),

$$\psi_{nL}^* = \lambda(\ln \sqrt{R_+^*} - \ln \sqrt{R_-^*}), \tag{12}$$

where $R_\pm^*$ and the non-dimensional coefficient λ are defined by the relations

$$R_\pm^* = x^{*2} + (y^* \pm 1)^2 + \xi, \quad \lambda = \frac{\Gamma}{2\pi a V_\ell}. \tag{13}$$

Numerical values of the parameter λ are illustrated below in Table III.

The non-dimensional form of Eq. (6) is

$$\frac{d\mathbf{u}_p^*}{dt} = \frac{1}{\mathrm{St}}(\mathbf{v}_n^* - \mathbf{u}_p^*) + \frac{3\rho_n}{2\rho_o}(\mathbf{v}_n^* \nabla^*)\mathbf{v}_n^* + \frac{3\rho_s}{2\rho_o} C_s \nabla^* \frac{1}{r*^2}, \tag{14}$$

where ∇^* is the gradient operator in $(x^*,\ y^*)$-space; the Stokes number, St and the parameter C_s are defined as

$$\mathrm{St} = \frac{V_\ell \tau}{a}, \quad C_s = \frac{\kappa^2}{8\pi^2 a^2 V_\ell^2} = \frac{1}{2}\left(\frac{\kappa}{\Gamma}\right)^2 \lambda^2. \tag{15}$$

TABLE III

Parameters λ and C_s.

V_s (cm/s)	0.01	0.01	0.01	0.01	0.1	0.1	0.1	0.1
T (K)	1.3	1.5	1.8	2.1	1.3	1.5	1.8	2.1
λ	0.0905	0.186	0.328	0.197	0.0724	0.159	0.258	0.111
C_s	1.324	1.392	1.415	0.999	0.0132	0.0137	0.0137	0.0105

For neutrally buoyant particles, in Eq. (14)

$$\frac{3\rho_s}{2\rho_o} = \frac{\rho_s}{\rho} = B \quad \text{and} \quad \frac{3\rho_n}{2\rho_o} = \frac{\rho_n}{\rho} = 1 - B. \tag{16}$$

In non-dimensional variables, the form of the kinematic equation (9) remains unchanged.

For various V_s and T, the Stokes number can be calculated from formulae (15) and (7) using Table I which shows the superfluid line velocity V_ℓ as a function of the externally applied superfluid velocity and temperature, and properties of helium II reported in Ref. 15. For neutrally buoyant particles of radii typical of PIV applications in helium II, the Stokes number lies in the interval from 10^{-5} to 10^{-2} (for example, $\mathrm{St} = 3.09 \times 10^{-5}$ for $1\,\mu$m particles at $T = 1.3\,\mathrm{K}$ and $V_s = 0.01\,\mathrm{cm/s}$, and $\mathrm{St} = 8.93 \times 10^{-3}$ for $5\,\mu$m particles at $T = 1.8\,\mathrm{K}$ and $V_s = 0.1\,\mathrm{cm/s}$.) Table III shows the values of the parameter C_s which does not depend on the particle properties.

Below we assume that at the initial moment, $t = 0$ the particle, situated sufficiently far from the triple-vortex system, has the velocity coinciding with that of the normal fluid, i.e. $\mathbf{u}_p = 0$ in the laboratory reference frame. Hence, in the reference frame of the vortices, the dimensionless velocity and position of the particle are:

$$\mathbf{u}_p^* = (-1, 0), \quad x_p^* = x_0, \quad y_p^* = y_0 \quad \text{at} \quad t = 0. \tag{17}$$

4. LAGRANGIAN TRAJECTORIES AND COLLISIONS OF SOLID PARTICLES WITH THE SUPERFLUID VORTEX: TRAPPING OF SOLID PARTICLES

The equations of motion (14) and (9) subject to initial conditions (17) were solved numerically. The non-dimensional initial distance x_0 from the vortex structure was chosen sufficiently large (in most calculations $x_0 = 5$) in order to eliminate an influence of the normal and superfluid flow on the initial motion of the particle. In the case where the initial distance y_0 from the axis Ox^* along the superfluid line velocity is sufficiently

large, the vortices and the jet in the normal fluid deflect the particle away from the triple-vortex structure thus preventing a collision of the particle with (and, therefore, a possible particle trapping on) the superfluid vortex. Typical trajectories illustrating the deflection of the neutrally buoyant particle of radius $a_p = 3 \times 10^{-4}$ cm are shown in Fig. 2. It can be seen that, even for rather small initial distances y_0 (0.063 in the case illustrated on Fig. 2 right), the normal fluid flow generated by the mutual friction is sufficiently strong to deflect even the considered relatively large particle away from the superfluid vortex (in Fig. 2 right the trajectory, originating at the same initial distance $y_0 = 0.063$, calculated neglecting the normal fluid disturbances induced by the mutual friction is also shown by the dashed line for comparison). As could be anticipated, in the case where y_0 is sufficiently small, the particle will collide with the core of the superfluid vortex located at $x^* = 0$, $y^* = 0$, so that the particle can be trapped provided the relative velocity between the particle and the superfluid vortex is not too large. Typical trajectories illustrating the phenomenon of trapping are shown in Fig. 3.

Before analyzing the quantitative parameters of particle–vortex collisions, we consider, in a rather qualitative manner, the time behavior of the main forces acting on the particle along its trajectory. The three terms in the right hand side of the non-dimensional equation of particle motion (14) represent, respectively, the Stokes viscous drag force $\mathbf{F}_n^{(d)}$, the inertial (added mass) force $\mathbf{F}_n^{(i)}$ exerted by the normal fluid, and the pressure gradient force $\mathbf{F}_s$ exerted by the superfluid vortex. Figure 4 illustrates the evolution with time of the magnitudes of these forces along typical trajectories. Time series shown on this figure correspond to $T = 1.8$ K and $V_s = 0.1$ cm/s, but the analysis below remains valid for all considered temperatures and externally applied superfluid velocities.

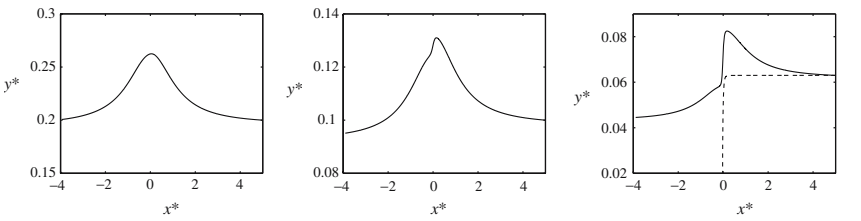

Fig. 2. Typical trajectories of the neutrally buoyant inertial particle deflected by the dipole-like vortex structure in the normal fluid as a function of initial position (left: $y_0 = 0.2$; middle: $y_0 = 0.1$; right: $y_0 = 0.063$; the trajectory calculated neglecting the normal flow disturbances is shown by the dashed line). The motion of the particle is from right to left. The vortex is at the origin. In all calculations $T = 1.8$ K, $V_s = 0.1$ cm/s, and $a_p = 3 \times 10^{-4}$ cm.

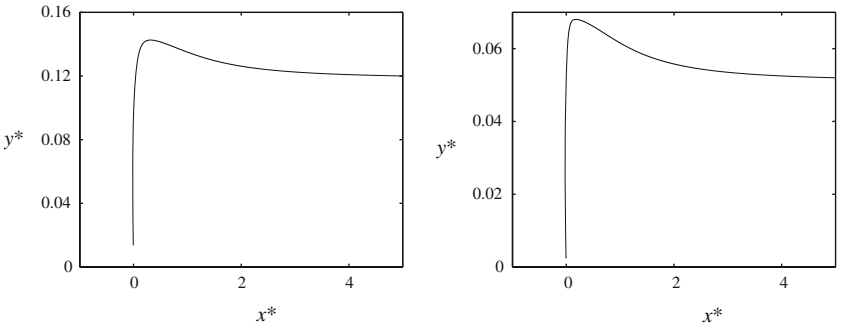

Fig. 3. Trajectories of the neutrally buoyant inertial particle illustrating its collision with the superfluid vortex located at $x=0$, $y=0$. The motion of the particle is from right to left. In all calculations $a_p = 3 \times 10^{-4}$ cm. Left: $T = 1.5$ K, $V_s = 0.01$ cm/s and $y_0 = 0.12$; right: $T = 1.8$ K, $V_s = 0.1$ cm/s and $y_0 = 0.052$.

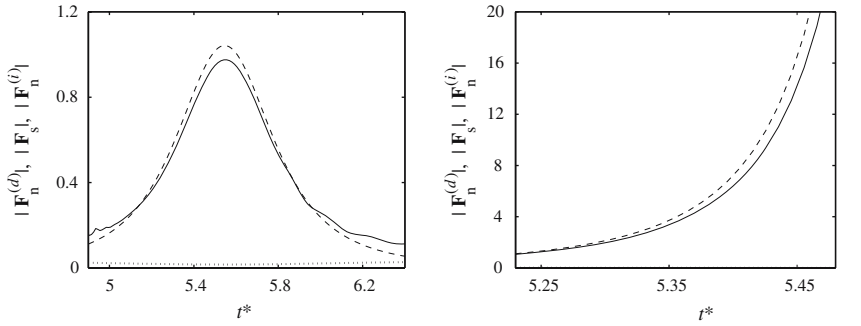

Fig. 4. Magnitudes of forces acting on the particle along its trajectory (t^* – non-dimensional time.) Solid line – normal viscous drag $|\mathbf{F}_n^{(d)}|$; dashed line – force $|\mathbf{F}_s|$ exerted by the superfluid vortex; dotted line – inertial force $|\mathbf{F}_n^{(i)}|$ exerted by the normal fluid. In all calculations $T = 1.8$ K and $V_s = 0.1$ cm/s. Left (for the particle trajectory shown on Fig. 2 (left), $a_p = 3 \times 10^{-4}$ cm, $y_0 = 0.2$): deflection of the particle by normal fluid disturbances. Right: particle–vortex collision ($a_p = 5 \times 10^{-4}$ cm, $y_0 = 0.06$).

The case where the particle is deflected by the normal fluid disturbances is illustrated in Fig. 4 (left) corresponding to the trajectory shown in Fig. 2 (left) for $a_p = 3 \times 10^{-4}$ cm and $y_0 = 0.3$. For most of time the magnitude of the viscous drag force, deflecting the particle away from the superfluid vortex core, remains larger than that of the pressure gradient force exerted by the superfluid vortex, except for the relatively short time interval during which the particle is closest to the vortex core and the force exerted by the superfluid vortex dominates. However, this does not mean that the particle will accelerate towards the vortex core and collide,

eventually, with it. The radial component (in cylindrical coordinates of the superfluid vortex) of this force plays a rôle of the centripetal force keeping the particle on its curvilinear trajectory around the vortex core. Because the particle does not collide with the superfluid vortex, this force remains finite at all times.

In the case where the particle collides with the superfluid vortex, initially the magnitude of the viscous drag force dominates the pressure gradient force, but as the particle approaches the superfluid vortex closer, the force exerted by the superfluid vortex becomes larger than the other two forces and then grows infinitely as the moment of collision is approaching. The magnitude of the viscous drag force also tends to infinity as the particle accelerates towards the superfluid vortex core, but slower than the force exerted by the superfluid vortex. The behavior of magnitudes of forces shortly before the particle–vortex collision is shown on Fig. 4 (right); for convenience of illustration, the evolution of forces along the particle trajectory is shown in this case for slightly larger particle size, $a_p = 5 \times 10^{-4}$ cm; here $y_0 = 0.06$.

In the both considered cases, during the time interval when the particle is relatively close to the vortex the inertial force $\mathbf{F}_n^{(i)}$ exerted by the normal fluid disturbances remains smaller than the other two forces and does not play any significant rôle in the particle–vortex interaction.

Below we define the dimensionless impact parameter as $\Delta = 2(y_0)_{cr}$, where $(y_0)_{cr}$ is the non-dimensional critical initial distance from the axis Ox^* separating the two regimes of motion, one where the particle is deflected by the normal vortices, and the other where the particle collides with the superfluid vortex and can be trapped, eventually, by its core. Thus, in our two-dimensional model, the parameter Δ plays the rôle of the cross-section of particle–vortex collision. For example, the trajectory in Fig. 2 (right) illustrates the case where the initial coordinate y_0 is only slightly larger than $(y_0)_{cr}$.

For neutrally buoyant particles, the dimensionless impact parameter Δ is a function of the Stokes number St and the non-dimensional parameters λ, C_s, and $B = \rho_s/\rho$ defined by formulae (13), (15) and (16). It is important to notice that it is only the Stokes number that contains the properties of the solid particle. The parameters λ and C_s depend only on the properties of helium II and those of the vortex structure, so that they are functions of temperature T and applied superfluid velocity V_s. The parameter B is, of course, a function of temperature alone. In order to analyze an influence of the particle properties on the dimensionless impact parameter Δ, the latter is represented in Fig. 5 as a function of the Stokes number for $V_s = 0.01$ and $V_s = 0.1$ cm/s and temperatures $T = 1.5$, 1.8, and

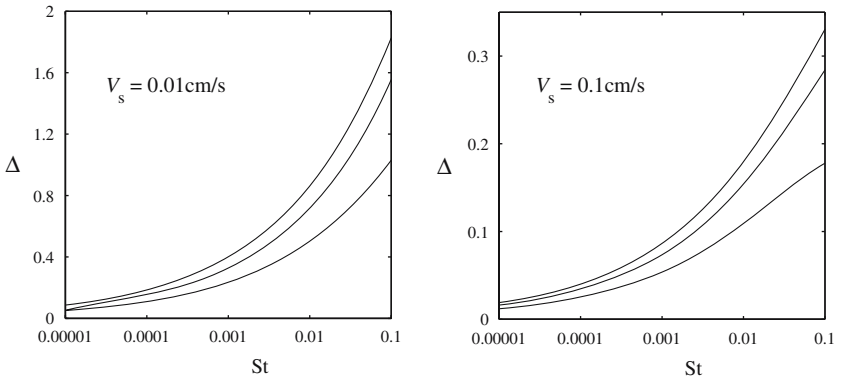

Fig. 5. Non-dimensional impact parameter Δ as a function of the Stokes number $\mathrm{St} = V_\ell \tau / a$. Curves from top to bottom: $T = 1.5$, 1.8, and 2.1 K.

2.1 K (the properties of He II are taken from the work by Donnelly and Barenghi,[15] and the properties of the triple-vortex structure from the data shown in Tables I and II). It can be seen from Fig. 5 that at relatively large Stokes numbers the dimensionless impact parameter Δ increases rapidly with St but remains much less sensitive to changes in St if the Stokes number is smaller than $\sim 10^{-4}$. It should be remembered that the Stokes number is proportional to a_p^2, so that for very small particles the viscous drag becomes large compared to all other forces and, in particular, dominates the pressure gradient force induced by the superfluid vortex, unless the particle approaches the superfluid vortex core very closely (it can be said that a very small, neutrally buoyant particle moves almost as a normal fluid point). This explains small the values of Δ, which are relatively insensitive to changes in the Stokes number. On the other hand, for larger particles the ratio of the force exerted by the superfluid vortex to the viscous drag force becomes significant at much larger distances; for a fixed distance, this ratio increases with the particle size as a_p^2. This explains a rapid increase of Δ with St as the Stokes number becomes larger than $\sim 10^{-3}$.

Since the non-dimensional parameters other than St do not depend on the particle properties, i.e. $\lambda = \lambda(T, V_s)$, $C_s = C_s(T, V_s)$, and $B = B(T)$, it would be more convenient and informative to illustrate directly the dependence of the dimensionless impact parameter of particle–vortex collision on temperature. Figure 6 shows Δ as a function of T for the neutrally buoyant particle of the size $a_p = 1\,\mu$m for two superfluid velocities, $V_s = 0.01$ cm/s and $V_s = 0.1$ cm/s. It can be seen that the dimensionless impact parameter decreases with temperature; this decrease becomes more

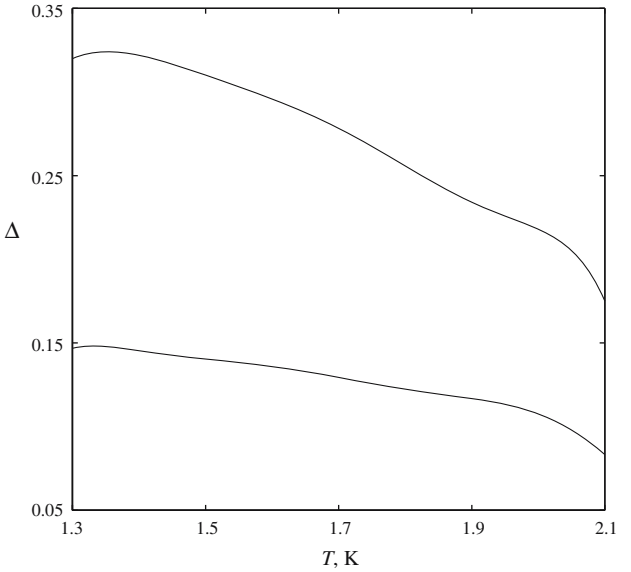

Fig. 6. Impact parameter as a function of temperature; $a_p = 10^{-4}$ cm, $\rho_p = 0.145\,g/cm^3$. Top: $V_s = 0.01$ cm/s; bottom: $V_s = 0.1$ cm/s.

significant in the vicinity of the λ-point where the density of the normal fluid becomes higher and the force exerted on the particle by the superfluid vortex relatively less significant.

In conclusion of this section, we will give a qualitative explanation of how the properties of the fluid and the particle affect the impact parameter of particle–vortex collision. The impact parameter is controlled by the balance of the pressure gradient force attracting the particle to the superfluid vortex core, and the viscous drag force sweeping the particle away from it. The former force is represented by the third term, while the latter by the first term in the right-hand sides of Eqs. (6) and (14). Using formulae (7) and (15) and taking into account that $V_\ell \approx V_s$ (see Table I), the ratio of these forces can be easily estimated from the non-dimensional equation (14) as

$$\frac{3\rho_s C_s \mathrm{St}}{2\rho_o} \approx \frac{\kappa^2}{24\pi^2 a^2} \frac{\rho_s a_p^2}{\mu_n V_s}. \tag{18}$$

Clearly, the region, where the particle is likely to collide with the superfluid vortex core, and, therefore, also the impact parameter Δ will increase with the ratio in Eq. (18). From Eq. (18) it follows that the impact parameter must grow rapidly with the particle size and decrease with the

externally applied superfluid velocity V_s, as can indeed be seen from Fig. 5. The temperature dependence of the estimate (18) is controlled by the ratio ρ_s/μ_n. The latter, easily calculated from the data reported in Ref. 15, has a maximum between $T = 1.4$ and $T = 1.5\,\mathrm{K}$ and decreases monotonically for higher temperatures. This behavior corresponds to the temperature dependence of the impact parameter shown in Fig. 6 (the maximum of the curves in Fig. 6 does not correspond exactly to the maximum of ρ_s/μ_n because in the estimate (18) the temperature-dependent superfluid line velocity V_ℓ has been replaced by the constant externally applied velocity V_s.)

5. PARTICLE–VORTEX COLLISIONS IN THE CASE WHERE THE PEAK NORMAL VELOCITY AND THE SUPERFLUID LINE VELOCITY ARE NOT ALIGNED

Although we assumed above that the peak normal velocity, $\mathbf{v}_{n0}$ and the velocity of the vortex structure, $\mathbf{V}_\ell$ are perfectly aligned, in general it is not the case, and the angle θ, sketched in Fig. 7, is a function of temperature and superfluid velocity, $\theta = \theta(T, V_s)$. As was found in Ref. 6, θ is a decreasing function of temperature; in particular, $\theta \approx 0.2\pi$ and $\theta \approx -0.25\pi$ at $T = 1.2$ and $T = 2.1\,\mathrm{K}$, respectively (θ is close to zero in the vicinity of $T = 1.6\,\mathrm{K}$). However, θ decreases rapidly as the temperature approaches the λ-point ($\theta \approx -0.4\pi$ at $T \approx T_\lambda$). Although in the temperature interval

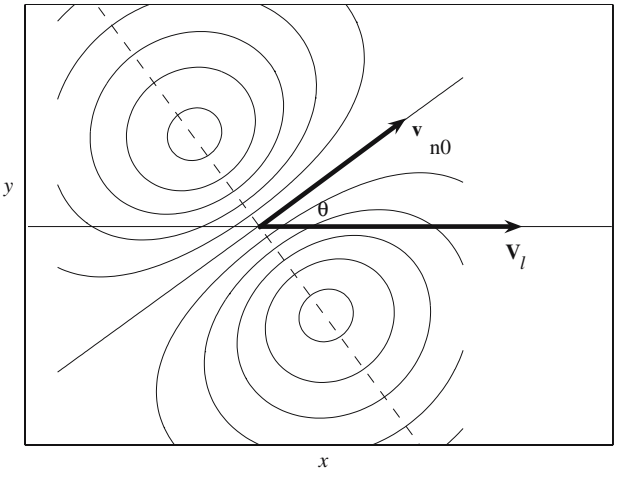

Fig. 7. Schematic representation of the triple-vortex structure in the case where the peak normal velocity and the superfluid line velocity are not aligned.

between $T = 1.2$ and $T = 2.1\,\mathrm{K}$ the angle θ is not large, it seems useful to estimate whether this tilt of the normal vortex dipole with respect to $\mathbf{V}_\ell$ has any significant influence on the results discussed in the previous section.

The generalization of the model (2)–(4) (or (11)–(13), in the non-dimensional variables) for the flow generated by the "tilted" normal fluid dipole is trivial and will not be discussed here in detail. Particle trajectories originating at $y^* = y_0$ and $y^* = -|y_0|$ are no longer symmetric with respect to the axis Ox, so that the critical distance in the upper half-plane, $(y_0)^+_{\mathrm{cr}} > 0$ (such that the particle will collide with the superfluid vortex provided the initial y-coordinate $y_0 < (y_0)^+_{\mathrm{cr}}$) does not coincide with the magnitude of the critical distance in the lower half-plane, $|(y_0)^-_{\mathrm{cr}}|$). Figure 8 shows typical trajectories of the neutrally buoyant $3\,\mu$m-size particle in the case where the initial distance $|y_0|$ exceeds only slightly either $(y_0)^+_{\mathrm{cr}}$ or $|(y_0)^-_{\mathrm{cr}}|$. The trajectories in the case where the angle θ is assumed to be zero are shown by dashed lines for comparison. The calculations show that, for example, at $T = 1.3\,\mathrm{K}$ the "positive" critical initial distance, $(y_0)^+_{\mathrm{cr}}$ is smaller, while the "negative" critical distance $|(y_0)^-_{\mathrm{cr}}|$ is larger by about 45% than the value $((y_0)_{\mathrm{cr}})_{\theta=0}$ calculated for $\theta = 0$. At $T = 2.1\,\mathrm{K}$, $(y_0)^+_{\mathrm{cr}}$ is larger, and $|(y_0)^-_{\mathrm{cr}}|$ is smaller by $\sim$55% than $((y_0)_{\mathrm{cr}})_{\theta=0}$. At intermediate temperatures the difference between $(y_0)^+_{\mathrm{cr}}$, $|(y_0)^-_{\mathrm{cr}}|$ and $((y_0)_{\mathrm{cr}})_{\theta=0}$ becomes smaller and vanishes in the vicinity of $T \approx 1.6\,\mathrm{K}$.

Clearly, in the case where $\theta \neq 0$ the impact parameter must be defined as

$$\Delta = (y_0)^+_{\mathrm{cr}} + |(y_0)^-_{\mathrm{cr}}|. \tag{19}$$

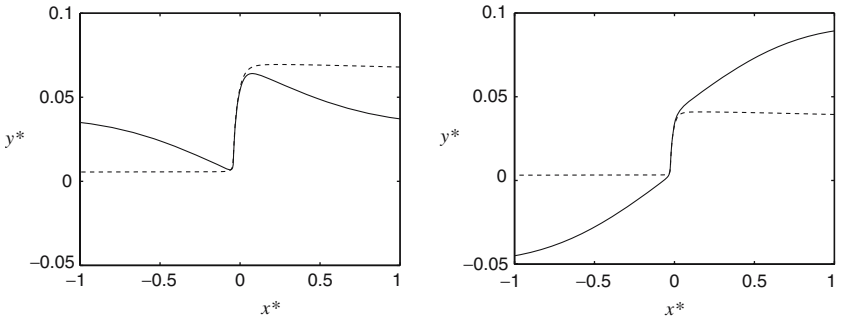

Fig. 8. Typical trajectories of the neutrally buoyant particle in the case where the initial distance $|y_0|$ only slightly exceeds either $(y_0)^+_{\mathrm{cr}}$ or $|(y_0)^-_{\mathrm{cr}}|$. In the case where the angle θ is assumed to be zero, the trajectories are shown by dashed lines for comparison. In all calculations $a_{\mathrm{p}} = 3 \times 10^{-4}\,\mathrm{cm}$. Left: $T = 1.3\,\mathrm{K}$, $\theta \approx 0.2\pi$; right: $T = 2.1\,\mathrm{K}$, $\theta \approx -0.2\pi$.

Surprisingly, the analysis of particle trajectories in the temperature interval from $T = 1.3$ to $T = 2.1\,\mathrm{K}$ shows that, although $(y_0)^{\pm}_{\mathrm{cr}}$ can differ quite significantly from $((y_0)_{\mathrm{cr}})_{\theta=0}$, the value of the impact parameter defined by relation (19) differs by less than 2% from the value of Δ calculated assuming $\theta = 0$. In the temperature interval between $T = 2.1$ and $T = T_\lambda \approx 2.17\,\mathrm{K}$ an influence of the temperature-dependent angle θ on particle trajectories and the impact parameter Δ becomes more pronounced. However, in the context of PIV studies of superfluid He II, the latter, rather small interval of temperatures is not of major interest, so that we will not pursue further the analysis of an influence of θ on particle trajectories.

6. CONCLUSIONS

Based on a simple two-dimensional model of the triple-vortex structure consisting of the superfluid vortex and the vortex dipole in the normal fluid, we analyzed the Lagrangian trajectories of inertial particles interacting with this local vortex structure in superfluid helium II. We found that the normal vortices, induced by the mutual friction between the normal fluid and the superfluid vortex, can deflect the solid particle which otherwise would have collided with the superfluid vortex core. In the latter case, the particle can possibly be trapped by the superfluid vortex provided that the relative velocity between the particle and the vortex is not too large. We identified the non-dimensional parameters characterizing the particle trajectories. We found that the particle can either collide with the superfluid vortex or be deflected by the normal vortices depending on the initial distance y_0 between the particle and the axis through the core of superfluid vortex along the superfluid line velocity. We calculated the impact parameter Δ which, in our two-dimensional model, plays the rôle of the cross-section of particle–vortex collision, such that the particle will collide with the superfluid vortex provided $y_0 < \Delta/2$, and deflected by the normal vortices in the case where $y_0 > \Delta/2$. The impact parameter Δ is found to be a function of temperature, externally applied superfluid velocity, and the Stokes number combining the size of the triple–vortex system, superfluid velocity, and the particle response time, the latter determining an interaction between the particle and the viscous normal fluid at small particle Reynolds numbers. We have shown that for relatively large particles the impact parameter increases rapidly with the particle size but remains much less sensitive to the particle size for small particles. We have also analyzed the dependence of Δ on temperature. The considered model has also been generalized for the case where the peak velocity of the jet generated by the dipole-like structure in the normal fluid is not fully aligned with the velocity of the superfluid vortex;

the angle θ between these velocities is a function of temperature and the externally applied superfluid velocity. We have shown that this angle affects the impact parameter very little, except for the case where the temperature is in the close vicinity of the λ-point.

Given that the lengthscale of the normal flow disturbances induced by the mutual friction is expected to be only about 0.1 mm, there is no surprise that so far there was no direct experimental evidence of the nature of local vortex structures. The reason for that is poor spatial resolution of visualization techniques (such as second sound, ion trapping, measurements of temperature, pressure an chemical potential) most widely used prior to implementation of the PIV methods. Perhaps the results of this work may assist the future attempts to show experimentally, by means of the PIV technique, the existence of local vortex structures induced, in the normal fluid, by the mutual friction.

The model developed in this paper shows that, although the phenomenon of particle trapping by superfluid vortices is a serious issue that must be taken into account when interpreting results of PIV measurements in helium II, events of trapping are perhaps less frequent than could have been expected from the model that does not account for normal fluid vortices induced by the mutual friction.

ACKNOWLEDGMENTS

The research of YAS and CFB is supported by EPSRC Grant GR/T08876/0. The authors thank Dr. O. C. Idowu for providing the details of calculation of the local vortex structures in the normal fluid, Mrs. L. H. Doyles for her help in calculating particle trajectories in the case where the normal dipole-like vortex structure and the velocity of superfluid vortex are not fully aligned, and Dr. D. Kivotides for fruitful discussions.

REFERENCES

1. R. J. Donnelly, A. N. Karpetis, J. J. Niemela, K. R. Sreenivasan, W. F. Vinen, and C. M. White, *J. Low Temp. Phys.* **126**, 327 (2002); T. Zhang, D. Celik, and S. W. Van Sciver, *J. Low Temp. Phys.* **134**, 985 (2004); T. Zhang and S. W. Van Sciver, *Nat. Phys.* **1**, 36 (2005); G. P. Bewley, D. P. Lathrop, and K. R. Sreenivasan, Nature **44**, 588 (2006).
2. T. Zhang and S. W. Van Sciver, *J. Low Temp. Phys.* **138**, 865 (2005).
3. N. G. Berloff and P. H. Roberts, *Phys. Rev. B* **63**, 024510 (2000).
4. D. R. Poole, C. F. Barenghi, Y. A. Sergeev, and W. F. Vinen, *Phys. Rev. B* **71**, 064514 (2005).
5. H. E. Hall and W. F. Vinen, *Proc. Roy. Soc. London Ser. A* **238**, 215 (1956); W. F. Vinen, *Proc. Roy. Soc. London Ser. A* **242**, 493 (1957).
6. O. C. Idowu, A. Willis, C. F. Barenghi, and D. C. Samuels, *Phys. Rev. B* **62**, 3409 (2000).
7. D. Kivotides, C. F. Barenghi, and D. C. Samuels, *Science* **290**(5492), 777 (2000).

8. K. W. Schwarz, *Phys. Rev. Lett.* **49**, 283 (1982); *Phys. Rev. B* **38**, 2398 (1988).
9. R. G. K. Aarts and A. T. A. M. De Waele, *Phys. Rev. B* **50**, 10069 (1994).
10. D. C. Samuels, *Phys. Rev. B* **47**, 1107 (1993).
11. C. F. Barenghi, D. C. Samuels, G. H. Bauer, and R. J. Donnelly, *Phys. Fluids* **9**, 2361 (1997).
12. D. Kivotides, C. F. Barenghi, and Y. A. Sergeev, *Phys. Rev. Lett.* **95**, 215302 (2005).
13. The data of this table, used in preparation Dr. Idowu's Ph.D. Thesis (University of Newcastle, 2000) and work [6] for publication, have been supplied by Dr. O. C. Idowu.
14. O. C. Idowu, D. Kivotides, C. F. Barenghi, and D. C. Samuels, *J. Low Temp. Phys.* **120**, 269 (2000).
15. R. J. Donnelly and C. F. Barenghi, *J. Phys. Chem. Ref. Data* **27**, 1217 (1998).